Low Cost Fabrication Of EU: Cds/Pbs Heterostructures

N.Kavitha, R. Chandramohan, A. Mohamed Haroon Basha, K.K. Sivakumar and R. Swaminathan

Abstract: The n type CdS with different doping level of Europium and p type PbS heterojunction solar cell was fabricated using Chemical Bath Deposition. CdS window layer was deposited on Indium tin Oxide (ITO) glass with 1% and 3% doping concentration of Europium. PbS absorber layer of thickness around 0.9 micron was grown on ITO/CdS to fabricate the p–n junction. The prepared three films were analyzed by X-ray diffraction, scanning electron microscopy (SEM), energy dispersive X-Ray spectroscopy (EDS), UV-Vis spectroscopy and photovoltaic studies. The photovoltaic properties including J–V characteristics, short-circuit current (Isc), open-circuit voltage (Voc), fill factor (ff), efficiency (η) of CdS/PbS heterojunction cells have been as well examined. The results show that increasing the doping level of Europium on CdS improved the performances of the fabricated photovoltaic cells A high efficiency was observed at 3 % doping of Eu in CdS.

Keywords : CdS thin film, Europium doping, structural, optical, photovoltaic properties

1. INTRODUCTION

THE Cadmium sulphide (CdS) is a II-VI wide direct band gap semiconductor and can be used in thinfilm Photo conductive devices, solarcells, photo detectors, transistors, and light emitting diodes. The high transmittance and moderate band gap (2.42 eV) possessed by CdS make it a suitable candidate for the fabrication of solar cells especially as an efficient window layer [1]. Cadmium sulphide (CdS) can form heterojunction photovoltaic cells with many materials like copper indium diselenide/sulphide, cadmium telluride (CdTe), and copper indium gallium de selenide/sulphide (CIGS) respectively [2]. It can also be used as a window layer with PbS to form photovoltaic cell. Hence, the CdS/ PbS structure can be used as energy converting interface. The n-type CdS serve as a window layer and transmits light which is absorbed in the p-type PbS absorbent layer. This generates hole-electron pairs at the interface. The photo generated electron–hole pairs are separated in the depletion region of CdS/PbS heterojunction [3] and creates a potential. The first CdS based solar cell was deposited by vapor transport deposition [4]. Interestingly, an efficiency of 21.7% was reported for CIGS devices with CdS layers grown by chemical bath deposition [2]. Use of RF sputtered CdS in CdTe solar cells resulted in an efficiency of 15.8% [5,6]. A 14.2% efficient thin film CdTe solar cell with CdS was deposited by (CSS) close-spaced sublimation [7]. Thin films of CdS can be formed as a single phase material by vapor phase methods. However, it has been studied using variety of techniques such as chemical deposition [8], spray pyrolysis [9], chemical vapor transport [10], Sucessive ionic layer absorption and reaction [11], magnetron sputtering [2,12], electron beam evaporation [13], and electro-deposition [14]. Each technique has its own advantage and disadvantage to produce quality thin films. Though there are a variety of techniques, researchers are more interested in a method which is more economical, expedient for large area deposition of highly smooth and uniform films well adhered to the substrates. In this report pure and Eu doped CdS, and PbS thin films are prepared by chemical bath deposition method and their structural, morphological, optical and photovoltaic studies have been analyzed.

- *Correspondence Author*
- *R. Chandramohan*, Department of Physics Vidya giri arts and Science College, Puduvayal, India.*
- *Md Haroon Basha, Department of Physics, AMET University, Chennai, India. Email: harunbasha09@gmail.com*
- *K.K. Sivakumar, Department of Chemistry, AMET University, Chennai. India. Email sivakumarccet@gmail.com*
- *N. Kavitha, Department of Physics, Vikram Engineering College, Madurai. India.*

2. EXPERIMENTAL PROCEDURE

2.1 Chemical and solution preparation

Analytical grade CdCl2 (0.005 mol/L) and NH4Cl were dissolved in 100 mL deionized water at room temperature. When heating the solution at 70 ºC a 0.04 mol/L of ammonia solution was added and stirred for 5 min, and finally 0.03 mol/L of thiourea was added to the solution. Cleaned glass slides used as substrates were placed vertically in the reaction bath and kept for a period of 60 minutes. After the set period the substrates were removed and cleaned with deionized water. In the bath, the added ammonia combines with Cd2+ and forms Cd(NH3)42+complex which releases Cd2+ions. Thiourea releases S2−ions as a sulfur source. Similar method was adopted for the preparation of 1% and 3% Eu-doped CdS thin films For the preparation of solar cells, PbS thin film was deposited on CdS coated (ITO) Indium tin Oxide substrates (sheet resistance of ITO is 10 Ω/sq). A 50 ml solution of 0.15M lead nitrate [Pb(NO3)2] and 0.1 M thiourea [SC(NH2)2] was used for the deposition of PbS. The alkalinity of the solution was set using 0.5 M sodium hydroxide [NaOH]. The CdS coated ITO substrate was vertically immersed into the solution and the beaker containing the reactive solution was kept in a water bath maintained at 60 °C for 1 hr.

2.2 Characterization

Thickness of the prepared films was measured using Alpha-step surface profiler. Structural property was analysed using X-ray diffraction pattern obtained using X'pert PRO (PANalytical) diffractometer with CuKα radiation (k = 0.15405 nm) in steps of 0.1 over the 2θ range of 10–80°. Morphological examination of the films was done using Hitachi (S-3000H) scanning electron microscope. In order to determine the band gap energy of the films, optical transmission study was carried out using Perkin Elmer Lambda 35 spectrophotometer. Photocurrent–voltage measurements were performed using Keithley 4200 semiconductor parameter analyzer under AM1.5G illumination

at 100 mW/cm2.

3 RESULTS AND DISCUSSION

3.1 X ray and structural analysis

Fig. 1 shows the X-ray diffraction patterns of undoped CdS, Eu doped CdS and PbS films prepared with the deposition time of 1 hr. The diffraction peak observed at 26.57° corresponds to (002) plane parallel to the substrate surface. This is an evidence for the preferential orientation along c-axis which is perpendicular to the substrate, a direction more favorable due to lowest surface energy [15]. The undoped and doped CdS thin films are formed in hexagonal crystal structure. The obtained XRD pattern agrees well with JCPDS card no. 41-1049. No extra peaks corresponding to Cd, Eu and sulphide related secondary and impurity phases are obtained attributing the complete incorporation of Eu ion into Cd lattice site. This XRD result also confirms the heterogeneous reaction of ion by ion deposition process which have resulted uniform hexagonal single phase CdS thin films [19].The narrow peak without doping concentration dependent shift indicates good crystallinity of deposited films. The XRD pattern of PbS also shows growth of good crystalline PbS displaying four characteristics peaks corresponding to (1 1 1), (2 0 0) (2 2 0) and (311) orientations in agreement with the standard JCPDS card No. 00-0050592 with cubic rock salt (NaCl) type structure [16]. The crystallite size (D) of CdS thin films were estimated using Scherrer's formula [17].

…….. (1)

Where D is average crystallite size, β is the full width at half maximum (FWHM),λ is the wavelength of x-ray whose value is 1.5418 Å (CuKa), K the Scherrer constant, which generally depends on the crystallite shape and is close to 1(K = 0.9 was used) and θ is the Bragg angle at the center of the peak. The crystallite size obtained from this equation corresponds to the mean minimum dimension of a coherent diffraction domain. It is found that the crystallite size calculated from (0 0 2) peak of CdS is increased from 28 nm to 35 nm for undoped to 3% Eu doped CdS respectively. The calculated crystallite size and other parameters of the CdS and PbS films are shown in Table 1. Dislocation density (δ) was calculated from crystallite size using equation (2) [16, 18].

$$\delta = \frac{1}{D^2}$$ …… (2)

Also strain (ε) of cadmium sulfide (CdS) film was calculated using the equation (3) [18]

$$\varepsilon = \frac{\beta \cos\theta}{4}$$

…….. (3)

The variation of dislocation density of undoped and Eu doped CdS thin films are given in table 1. It is observed from the Table.1 that the dislocation density and micro-strain is decreased by Eu-doping up to Eu 3%. The decrease of strain causes the increase of lattice parameters and average crystal size. This decrease of micro strain is responsible for the reduction of diffraction peaks [19, 20]. The relation connecting stacking fault probability (α) with peak shift Δ (2θ) is shown in the equation (3).

$$\alpha = \left|\frac{\Delta w}{\tan\theta}\right| \left|\frac{\Delta(2\theta)}{\Delta\theta}\right|$$

…….. (4)

Using the expression (4) the stacking fault probability was calculated by measuring the peak shift with the standard value. The intensity of the prominent peak (002) is found to increase as the film thickness increases.

3.2 Morphological studies

The variation in surface microstructure of CdS thin films as a function of Eu doping concentration obtained from SEM analysis is presented in Fig. 2(a–c). Fig. 2(a) shows that the surface microstructure of undoped CdS thin films consists of uniformly distributed spherical shaped particles. Fig. 2(b–c) shows the surface microstructures obtained from the films doped with 1% and 3% Eu concentrations respectively. Improved particle size and enhanced surface uniformity were observed in the films doped with 1% Eu and 3% Eu (Fig. 2(b) and (c), respectively).When the doping concentration increased to 3% Eu, the ad-atoms move over the surface, join together and get enlarged form sub grain collections resulting in the formation of bigger grains with good compactness [21]. Comparing the SEM images of the films grown at undoped and Eu doped CdS films the grains sizes of the films are increased as doping concentration increases. The SEM image shown in Fig. 2d shows surface of the PbS film grown on CdS. It shows spherical nano grains coated over the CdS. The elemental analysis of PbS-CdS thin films deposited on ITO substrate was performed using EDS energy dispersive X-ray analysis. The EDS spectrum Fig.2e shows the trace of Cd, Pb and S, thus confirmed the growth of CdS and PbS .

3.3 Optical studies

Optical behavior of materials are studied by UV-Vis-NIR spectroscopy. The optical transmittance spectra of the Eu-doped CdS thin films recorded in the wavelength region 400–1100 nm is shown in Fig. 3. It is clear that all films are highly transparent in the visible wavelength range and sharp ultraviolet absorption edge is observed at approximately 550 nm in the UV region. In Fig. 3 the inset shows transmittance spectrum of PbS film and it shows a value of transmittance around 25%. The optical absorption spectra of undoped and Eu doped thin films are recorded at room temperature from 400 to 1000 nm as shown in Fig. 4. This absorption spectrum shows that the absorption is high in the blue region of visible spectrum. The inset Fig. 4 shows absorption spectrum of PbS film and it shows a higher absorption in the visible region. Tauc's relation (relation between absorbance and band gap) describes the dependence of optical density with wavelength and band gap as well as nature of optical transition [22].

$$(\alpha h\upsilon)=B(h\upsilon - E_g)^{1/2}$$ …… (5)

Here, A is the characteristics independent constant, n is a constant number that depends on the nature or type of optical transition, hv is the photon energy, Eg is the energy band gap and α is the absorption coefficient. The constant number (n) has value ½ for direct transition and direct band gap optical materials like CdS [13, 22]. The E_g values of undoped and Eu doped CdS films determined from the Fig. 5 are found to be 2.47 and 2.5 eV respectively. These values of CdS band Fig.5 Inset shows Energy Band gap of PdS thin film gap are found

be in excellent agreement with the reported values in the literatures [23, 24]. Figure 5 inset shows the direct energy gap of PbS thin film deposited by nebulizer spray technique. The obtained band gap value of PbS is 1.56eV which is perfectly matched with band gap value reported for PbS [25]. The variation of band gap between the Eu doped and undoped CdS thin films is small in the present study.The optical constants of undoped and Eu doped CdS thin films were evaluated using the following relations [26],

$$n^2 = N + (N^2 - n_a^2 n_s^2)^{1/2} \quad \text{..... (6)}$$

where,

$$N = \frac{(n_a^2 + n_s^2)}{2} + 2n_a n_s T$$

n_a, ns and n are the refractive indices of air, substrate, and the CdS films, respectively. T is the transmittance value at a particular wavelength.

$$k = \frac{\alpha\lambda}{4\pi}$$

Where, a,λ, k are the absorption coefficient, wavelength, and the extinction coefficient, respectively. Fig. 6 and Fig.7 show the variation of both n and k of CdS films deposited with different doping concentration. The refractive index of the films decreased with the increase of doping concentration. The extinction coefficient of the films varied in the range from 0.33 to 0.35.The value of refractive index and extinction coefficient of CdS are found be in excellent agreement with reported in the literatures [13, 27, 28].

3.4. Photovoltaic studies

The CdS based PV cells were fabricated with undoped and Eu doped CdS on ITO coated glass substrate by CBD method. The photovoltaic performances of the ITO/Eu-CdS/PbS/Al solar cells are shown in Figure 8. The open-circuit voltage (V_{oc}) is found to increase from 0.31 to 0.36 V and the short circuit current density (J_{sc}) is increased from 6.83 to 7.72 mA/cm ^{2} with the increase of doping concentration. These results revealed that as the doping concentration increases the open circuit voltage also increase. The fill factor (FF) and energy conversion efficiency (η) were calculated using the following equations [16, 29]

$$FF = \frac{V_{max} I_{max}}{V_{oc} I_{sc}} \quad \text{..... (8)}$$

Where the Vmax and Imax are the values of maximum voltage and maximum current. The efficiency η (%) is calculated from the relation.

$$\eta = \frac{I_{sc} V_{oc} FF}{P_{in}} X100\% \quad \text{..... (9)}$$

The efficiency of the solar cells was estimated to be 1.16, 1.32 and 1.51 % respectively for the undoped CdS and Eu doped CdS films (1% and 3%), respectively. It was lower than the values reported by Obaid et al. [30] and Borja et al. [31] for the fabricated solar cells using PbS/CdS. The results obtained in this work show that the efficiency of the PV cell can be increased by increasing the doping concentration of the films. Detailed parameters of the solar cells extracted from the I–V characteristics are listed in Table 2. This significant improvement in photovoltaic performance of the fabricated ITO/Eu-CdS/PbS/Al solar cells may be attributed to the following reasons: (1) the increased grain size can reduce the particle-to-particle hopping of the photo-induced carrier. (2) The improvement in the quality of the Eu doped CdS thin films without imperfections and defects, which may reduce the recombination of photo excited carriers resulting high power conversion efficiency. The results obtained in this study have shown an improvement comparing the earlier reports [29, 31].

3.5 Figures and Tables

Eu doping in CdS film	Thickness (μm)	Crystallite size (nm)	Dislocation density (δ × 10^{15} lines. m^{-2})	Micro Strain (ε x 10^{-3} $lines^{-2}.m^{-4}$)	Stacking fault probability (α) x 10^{-4}
0%	0.62	28	1.21	5.3	3.4
1%	0.70	32	0.94	4.6	3.1
3%	0.74	35	0.79	4.2	2.8
PbS	0.89	51	0.38	2.6	1.4

Table 1 *Structural parameters*

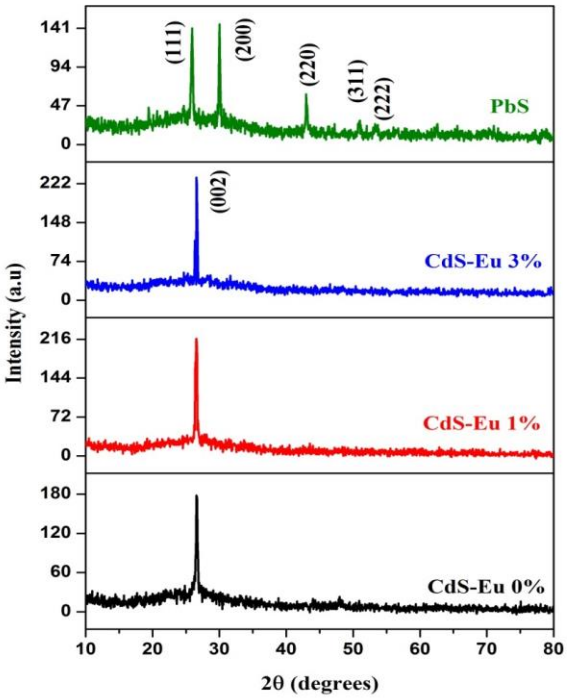

Fig.1*.XRD Pattern of Eu:CdS/PbS*

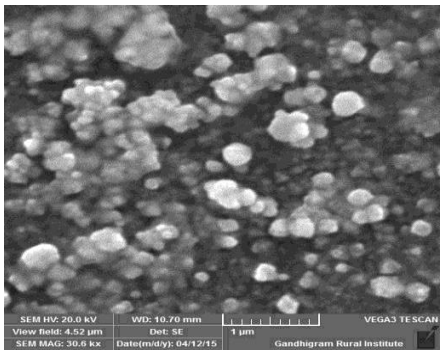

Fig.2*(a) Undoped CdS thin films*

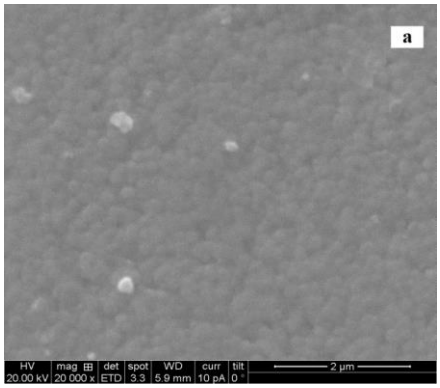

Fig.2*(b) 1%Eu doped CdS thin films*

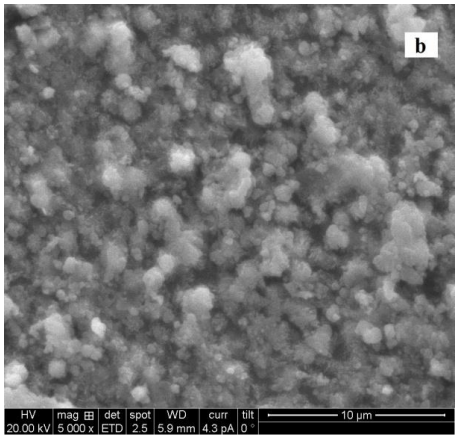

Fig.2*(c). 3% Eu doped CdS thin films*

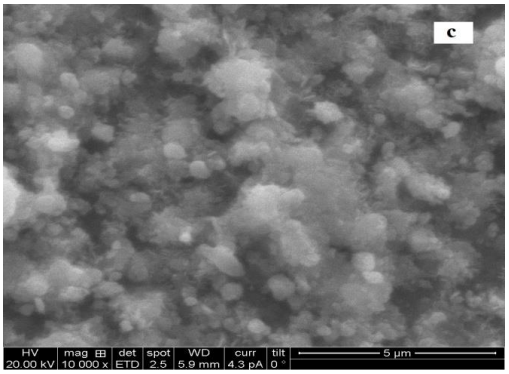

Fig.2*(d). PbS film grown on CdS*

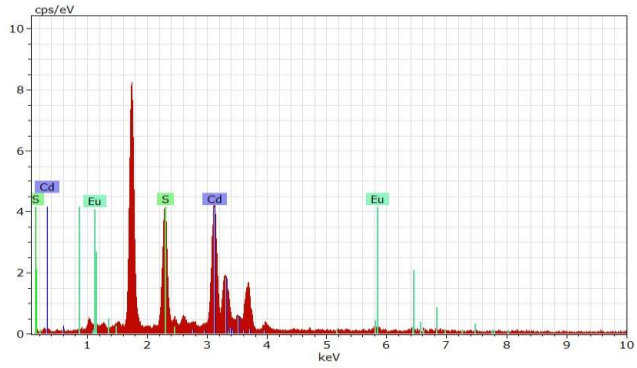

Fig.2*(e). EDS Spectrum*

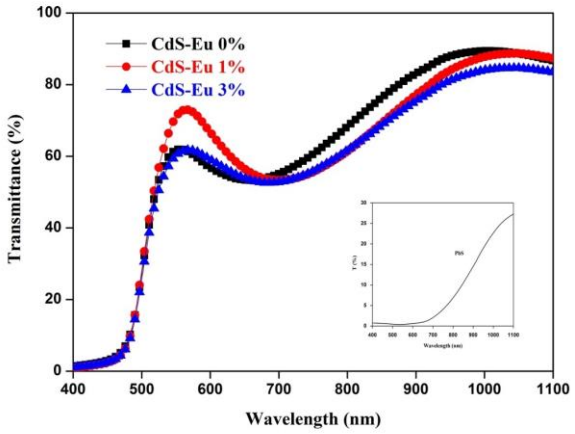

Fig.3 *Transmittance of Eu:CdS thin film*

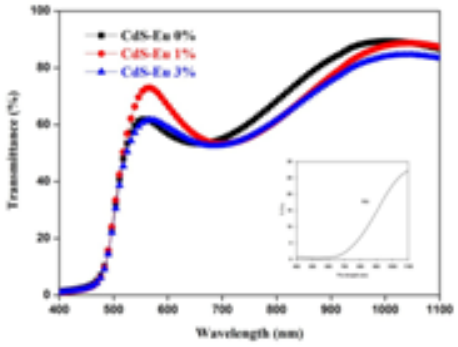

Fig.3 *Inset shows Transmittance of PdS thin film*

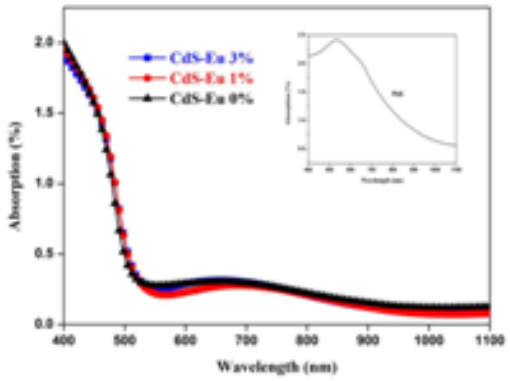

Fig.4 *Absorption spectra of Eu:CdS thin film*

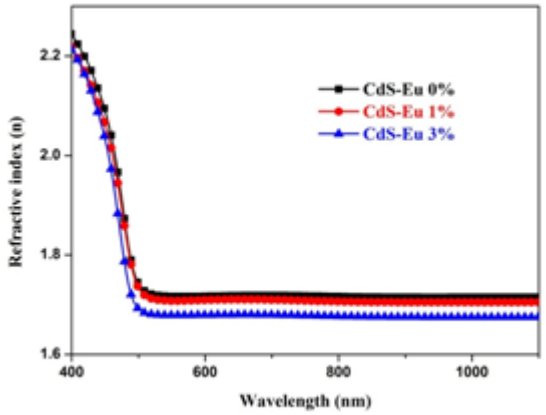

Fig.4 *Inset shows Absorption spectra of PdS thin film*

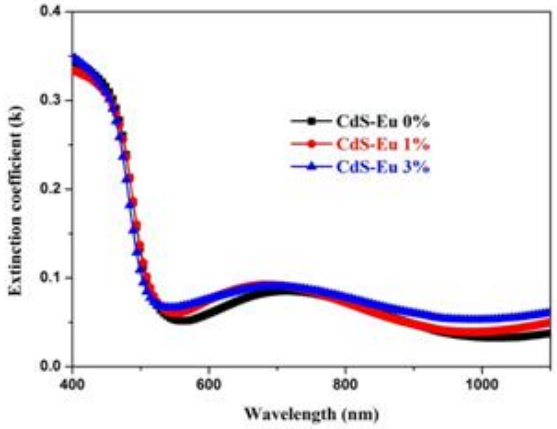

Fig.6 *Refractive Index Variation of Eu:CdS thin film*

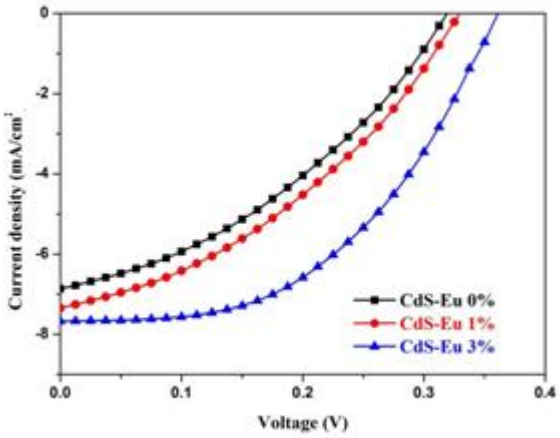

Fig.6 *Extinction Coefficient of Eu:CdS thin film*

Fig.8*. I-V Performances for Eu:CdS/PbS*

Table 2. *Solarcell Parameters of Eu doped CdS/PbS*

Parameters	Doping Concentrations		
	Eu 0%	Eu 1%	Eu 3%
V_{oc}(V)	0.31	0.32	0.36
I_{sc} (mA/cm^2)	6.83	7.32	7.72
FF	0.37	0.38	0.48
η (%)	1.16	1.32	1.51

CONCLUSION

CdS/PbS hetero structures were successfully prepared using chemical bath deposited PbS and chemical bath coated CdS layers. Europium doping with CdS has shown improved properties of the heterostructure. The CdS thin films have shown hexagonal phase with a preferred orientation in the (0 0 2) plane. PbS film has shown cubic rock salt structure with (200) preferred orientation. Crystallite size of the Eu doped CdS is found to increase with Eu concentration, and it is found to be 35 nm for the 3% Eu concentration.SEM analysis confirmed the crystallite grain size improvement with Eu concentration. Optical characterization showed a band gap variation from 2.47 to 2.5 eV for Eu doping concentration. Eu doping concentration is increased from 0% to 3% the solar conversion efficiency of the fabricated Eu: CdS/PbS solar cells is found to increase from 1.16 up to 1.51 % with the increase of Ru concentration. Though the results achieved are small they are obtained at crude conditions and can be improved by improving the measurement and fabrication conditions.

ACKNOWLEDGMENT

The authors wish to thank their Management and Senior members of Academy of Maritime Education and Training

(Deemed to be University), Chennai.

REFERENCES

[1] M. Anbarasi, V.S. Nagarethinam, R. Baskaran, V. Narasimman, Pacific Science Review A: Natural Science and Engineering, p. 1-6, 2016.

[2] F. Lisco, P.M. Kaminski, A. Abbas, K. Bass, J.W. Bowers, G. Claudio, M. Losurdo, J.M. Walls, Thin Solid Films, 582 , p .323-327, 2015.

[3] G.H. Tariq and M. Anis-ur-Rehman, Key Engineering Materials Vols, 510-511, p.156-162, 2012.

[4] Rapid Deposition Technology Holds the Key for World's Largest Solar Manufacturer, http://www.nrel.gov/awards/2003_hrvtd.html 2009 (Access date 2014).

[5] P. Kelly, R. Arnell, Vacuum, 56, 159. 2000.

[6] R.D. Arnell, P.J. Kelly, Surf. Coat. Technol., 112, 170, 1999.

[7] C.S. Ferekides, D. Marinskiy, S. Marinskaya, B. Tetali, D. Oman, D.L. Morel, Conference Record of the Twenty Fifth PVSC, p.751, 13–17, May 1996.

[8] H Moualkia, S Hariech, M S Aida, N Attaf1 and E L Laifa, J. Phys. D: Appl. Phys. 42 135404, 2009.

[9] A.A. Yadav, M.A. Barote, E.U. Masumdar, Solid State Sciences 12 , p.1173-1177, 2010.

[10] A Sanchez, P J Sebastian and 0 Gomez-Daza Sci. Techno., 10, p.87-90, 1995.

[11] K.M.Garadkar, A. A. Patil, P.V. Korake, P. P. Hankare Archives of Applied Science Research, 2 (5) ,429-437, 2010.

[12] Y H Sun, Y J Ge, W W Li, D J Huang, F Chen, L Y Shang, P X Yang1, and J H Chu, Journal of Physics: Conference Series 276, 012187, 2011.

[13] SubhashChander, M.S.Dhaka, Thin Solid Films, 638, p. 179-188, 2017.

[14] G. Sasikala, R. Dhanasekaran, C. Subramanian, Thin Solid Films 302, p.71- 76, .1997.

[15] C. D. G. Lazos, E. Rosendo, B. H. Juarez, G. G. Salgado, T. Diaz, M. R.Falfan, A. I. Oliva, P. Quintana, D. H. Aguilar, W. Cauich, M. Ortega, Y. Matsumoto J. Electrochem. Soc. 155, p.158- 162. 2008.

[16] N. Kavitha, R. Chandramohan, S. Valanarasu, T. A. Vijaya, S. Rex Rosario, A. Kathalingam, J Mater Sci: Mater Electron, 27, p. 2574-2580, 2016.

[17] P. Velusamy, R. Ramesh Babu, K. Ramamurthi, E. Elangovan, J. Viegas, M.S. Dahlem, M. Arivanandhan, Ceramics International 42, p. 12675–12685, 2016.

[18] KamaldeepKaur, Gurmeet Singh Lotey, N.K. Verma Materials Science in Semiconductor Processing 19, p.6–10, 2014.

[19] M. Muthusamy S. Muthukumaran, Optik - International Journal for Light and Electron Optics 126, p. 5200-5206, 2015.

[20] Pelleg, E. Elish, J. Vac. Sci. Technol. A 20 , p.754-761, 2002.

[21] M. Vasudeva Reddy, G. Sreedevi, Chinho Park, R.W. Miles, K. T. Ramakrishna, Reddy Current Applied Physics 15, 588-598, 2015.

[22] S. Yılmaz, S.B. Toreli, I. Polat, M.A. Olgar, M. Tomakin, E. Bacaksız, Materials Science in Semiconductor Processing 60, p. 45–52, 2017.

[23] Shadia J. Ikhmayies, Hassan K. Juwhari, Riyad N. Ahmad-Bitar, Journal of Luminescence 141, p.27–32, 2013.

[24] R. Premarani, J. JebarajDevadasan, S. Saravanakumar, R. Chandramohan, T. Mahalingam, , J Mater Sci: Mater Electron, 26 , p. 2059- 2065, 2015.

[25] A.S. Obaid, n , M.A. Mahdi, Z. Hassan, M. Bououdina, Materials Science in Semiconductor Processing 15, p.564–571, 2012.

[26] A. M. S. Arulanantham, S. Valanarasu, K. Jeyadheepan, A. Kathalingam, I. Kulandaisamy, J Mater Sci: Mater Electron,28, 13257, 2017.

[27] C. Santiago Tepantlan, Revista Mexicana De Fisica, 54 (2) , 112–117, 2008.

[28] H L pushpalatha, S. Bellappa, T N Narayanaswamy, R Ganesha, Indian Journal of Pure &Applied Physics, 52, 545-549, 2014.

[29] M. A. Barote, A. A. Yadav, T. V. Chavan, E. U. Masumdar, Digest Journal of Nanomaterials and Biostructures 6, p. 979-990, 2011.

[30] A.S. Obaid, M.A. Mahdi, Z. Hassan, M. Bououdin, Int. J. Hydrog. Energy 38, 807, 2013.

[31] J.H. Borja, Y.V. Vorobiev, R.R. Bon, Sol. Energy Mater. Sol.Cells 95, p.1882, 2011.